Available online at www.sciencedirect.com
ScienceDirect
Journal of the European Ceramic Society xxx (2014) xxx–xxx
www.elsevier.com/locate/jeurceramsoc

Feature Article

Segregation of anion (Cl^-) impurities at transparent polycrystalline α-alumina interfaces

Abhishek Tewari [a,*], Farhang Nabiei [b,c], Marco Cantoni [b], Paul Bowen [a], Cécile Hébert [b,c]

[a] Laboratory of Powder Technology, École Polytechnique Federale de Lausanne, CH-1015, Switzerland
[b] Centre Interdisciplinaire de Microscopie Electronique, École Polytechnique Federale de Lausanne, CH-1015, Switzerland
[c] Electron Microscopy and Spectrometry Laboratory, École Polytechnique Federale de Lausanne, CH-1015, Switzerland

Received 24 February 2014; received in revised form 10 April 2014; accepted 11 April 2014

Abstract

Small amounts of anion impurities (e.g. Cl), which are incorporated during the synthesis of ceramic powders, can affect the properties and microstructure of the final sintered ceramic. The effect of anion impurities is a little studied and poorly understood phenomenon. In this work a combination of STEM-EDX analysis and atomistic modeling approach was used to understand the segregation of Cl in transparent alumina ceramics. A high resolution analytical electron microscopy study showed the presence of Cl at the grain boundaries and especially at triple points. Atomistic simulations were carried out to understand the origins and consequences of such segregation. Segregation energy calculations predict a strong segregation of Cl at the different surfaces and grain boundaries of alumina. A higher coordination number of Cl at surfaces was observed, which indicates strong ionic bonds making it difficult to remove at low temperature, which explains the presence of Cl at triple points.

Keywords: Transparent alumina; Sintering; Segregation; Grain growth; Anion impurities

1. Introduction

α-Alumina powder has been used as a raw material for polishing abrasives, catalyst supports for high temperature reactions, cutting tools, and advanced ceramics. Powders of α-alumina are synthesized using several established methods, such as the Bayer process, calcination of gel based $Al(OH)_3$ in air or in controlled atmosphere, high temperature decomposition of aluminum-containing salts, and chemical vapor decomposition. Out of these methods, vapor decomposition method is employed very commonly to produce ultrafine α-alumina powders.[1,2] Synthesis of high purity alumina powders is crucial for the processing of advanced ceramic applications, e.g. transparent alumina.[3,4] Even a small amount of impurity could be detrimental for the performance of such advanced ceramics. There are several commercial α-alumina ultrafine powders available in the market, which claim to be 99.99% pure, e.g. Baikowski, Sumitomo. However, there are still small amounts of impurities present due to the synthesis process. Baikowski and Sumitomo, both report a total cation impurity (Na, Si, Fe, Ca etc.) content of ~50 ppm in their powders. However, none of the producers report any anion impurity content. In the literature also, there has been rarely any analysis done for the contents of anion impurities in alumina powders. Heuer et al.[5] determined 100 ppm anion impurity content using mass spectrometry in commercial alumina powders obtained from Johnsson Matthey and Co. Inc. New York. To the best of our knowledge there have not been any other attempts to quantitatively characterize the anion impurities in alumina. However depending upon the synthesis method, alumina can contain anion impurities from the precursors used in the synthesis i.e. Cl^- ions or $(SO_4)^{2-}$, something which is accepted by the majority of the people working in the field.

There are numerous studies available in the literature which focus on the effects of cation dopants/impurities on the properties of alumina, e.g. sintering and grain growth,[6] light

* Corresponding author at: MXD 334, Station 12, EPFL-STI-IMX-LTP, CH-1015 Lausanne, Switzerland. Tel.: +41 216 936 894; fax: +41 216 933 089.
E-mail address: abhit1985@gmail.com (A. Tewari).

http://dx.doi.org/10.1016/j.jeurceramsoc.2014.04.018
0955-2219/

transmission,[7] creep resistance.[8] However, the effects of anion impurities are very poorly understood, not only in the field of alumina, but also in the processing of other ceramic materials, like TiO_2, MgO, spinel etc. The very limited number of studies which are available throw some light on the importance of anion impurities in the processing of the ceramics. Fan et al.[9] reported that $C_2O_4^{2-}$ impurities in porous alumina membranes, accumulated during the electrochemical anodization process in oxalic acid solution, can affect its refractive index and adsorption coefficient. Roussel et al.[10] reported that doping with chloride salts of the dopants results into slightly higher sintered densities and real inline transmittance in alumina in comparison to the nitrate salts. But, no possible explanation was found for the better sintering with the chlorine salts. However, they also observed Cl in the secondary phase formed at the triple points of the La doped alumina grain boundaries in the EDX analysis of the samples in their later study.[11]

Leipold and Kapadia[12] studied the effect of anion impurities (S^{2-}, Cl^-, F^-, OH^-) on hot-pressing of MgO. It was reported that the final density of MgO is reduced due to the presence of all the anion impurities in the temperature range of 850–1150 °C. The vapor pressure and second phase precipitate formation at the interfaces were proposed to be the contributing factors behind the effects of anion impurities. However, no supporting evidence was reported for second phase precipitate formation.

Dittmann et al.[13] recently investigated the effect of Cl^- impurities on the sintering behavior of titania nano-particles. It was reported that although Cl^- impurities lowered the temperature of the anatase to rutile phase transition and densification, it resulted in a drastic grain growth during the final stage of sintering. Grain boundary (hereafter abbreviated as GB) embrittlement was also observed in the samples containing Cl^- impurities. It was proposed that the Cl^- anions get entrapped in the ceramic pore structure due to the early densification of titania nano powders. These pores cannot be closed during the final stage of sintering and result into the closed porosity in the dense ceramic.

In the light of these observations of effect of Cl on MgO and TiO_2 sintering and densification, the presence of such impurities may influence final microstructures and properties in other ceramics. In the quest to produce transparent polycrystalline alumina, powders produced via vapor phase synthesis with chloride precursors have shown significant promise.[6,14] However inhomogeneous grain growth[6] and residual porosity[14] have been observed, but the origin of such effects were not elucidated. From the work of Dittmann et al.[13] on Cl impurities in TiO_2, possible effects of Cl impurities in the transparent alumina were postulated as being a contribution and are investigated here. The present work is a combination of electron microscopy and atomistic modeling study of the segregation behavior of Cl in transparent polycrystalline alumina samples. Scanning transmission electron microscopy (STEM) and energy dispersive X-ray (EDX) analysis were used to characterize the Cl presence in optimized transparent alumina samples produced by SPS[6] (Section 3.1). Given the experimental complexity to observe the individual segregated interfaces in sintered ceramics, atomistic modeling can be a useful tool to study the segregation behavior of dopants/impurities in ceramics. Previously it has been used successfully in our group to study the segregation behavior of several cations on alumina interfaces.[15–17] In the present work, the energy minimization method was used in order to calculate the segregation energy of Cl on different alumina interfaces (Section 3.2). The coordination numbers of Cl^- ions on the interface were calculated in order to get an idea of the chemical environment of the ions on the interfaces (Section 3.4). Being a very little explored area of study, this preliminary work highlights the importance of anion impurities in the processing of advanced alumina ceramics and discusses ways to improve microstructural properties. In addition, if the findings of the atomistic modeling study can be validated with the microscopy observations, it can be used as a predictive tool for understanding the distribution of the anion impurities in the alumina microstructure.

2. Methods

2.1. Experimental method

The detailed procedure for the synthesis of Y-La doped transparent α-alumina samples, which have been used in this work for the electron microscopy analysis can be found in our earlier work.[6] Polyhedral near spherical Sumitomo α-Al_2O_3 powder with a median particle size Dv50 of 510 nm and total cation impurity concentration of less than 0.01% (less than 5 ppm for Si, Na, Mg, Cu and Fe) and a specific surface area S_{BET} of 4.2 m^2/g was used for the synthesis. Alumina powders were dispersed in 0.01 M HNO_3 solution before the dopants were added using the nitrate salts of both the dopants ($Y(NO_3)_3{\cdot}6H_2O$, $La(NO_3)_3{\cdot}6H_2O$) dissolved in 0.1 M HNO_3 solution. Therefore, the only source for Cl has to be the commercial powder itself, although no anion impurities were reported by the suppliers. The powder was spark plasma sintered at 1380 C and 100 MPa, producing real-in-line transmittance (RIT) of ~47% and average grain size ~0.96 μm.

The TEM specimen lamella were prepared using focused ion beam (FIB) with the thickness of about 350 nm. A FEI Tecnai Osiris Microscope operating at 200 kV with a Field Emission electron Gun (FEG) and equipped with four Super-X SDD EDX detectors was used for the microscopy analysis. Scanning transmission electron microscopy (STEM) in combination with energy dispersive X-rays (EDX) were used for imaging and analytical data acquisition. To get the exact amount of Cl at the GBs using the EDX analysis, first the GB is tilted edge-on and parallel to the optical axis. Then, data was acquired for about 1 h from the grain boundary. Because of lower number of pixels and higher acquisition time in these maps we get higher number of counts which makes it possible to observe the Chlorine composition contrast. Afterwards, a line scan is done perpendicular to each GB by summing up the counts for the pixels situated on a line parallel to the GB. This data is then quantified with the Esprit 1.9 software provided by Bruker corporation. Absorption

Please cite this article in press as: Tewari A, et al. Segregation of anion (Cl^-) impurities at transparent polycrystalline α-alumina interfaces. *J Eur Ceram Soc* (2014), http://dx.doi.org/10.1016/j.jeurceramsoc.2014.04.018

Table 1
Results of the Al–Cl Buckingham pair potential parameter optimization, the experimental and the fitted lattice parameter along with the error are listed in the table.

	A	B	C	α	β	γ
Fitted	3.43	3.81	8.58	90.0	90.0	90.0
Experimental	3.62	3.61	7.67	90.0	90.0	90.0
Error (%)	−5.2	5.5	11.9	0	0	0

correction for a sample thickness of ~350 nm was included in the extended Cliff-Lorimer quantification process. STEM-EDX compositional analysis was done on 7 chosen GBs in the alumina sample, which were straight and easy to orient edge on.

2.2. Computational method

The details of the segregation calculations can be found in our previous work on cation segregation on alumina interfaces.[15–17] The energies of the doped and undoped surfaces and GBs were calculated using the Born model for solids. The Born model describes the interatomic forces in terms of pair potentials. In this case, the pair potential parameters were taken from the work of Binks et al.[18] Binks potential parameters were fitted to chlorides, oxides and fluorides of various metals (Li, Na, K, Al, Zn, Ag, Co etc.), including Al_2O_3. However, the Buckingham potential parameters were not derived for Al–Cl interaction in that work. Therefore, Al–Cl Buckingham potential parameters were calculated in the present work by fitting it to the aluminum-oxy-chloride (AlOCl) lattice parameters, keeping all other parameters constant as given in the Binks potential set. The fitted lattice parameters as well as the experimental parameters are given in Table 1.

The screening method to avoid calculating the large number of possible configuration and select only highest probable configurations was similar to that described earlier in the case of cation segregation.[16,17] To maintain the charge balance of the system one Al vacancy was created for every three Cl atoms. Our previous work on Mg doping showed that the Mg substitutional defect and oxygen vacancies are not coupled and therefore should be treated independently.[17] Similarly, Cl substitutional defects (O_{Cl}) and the Al vacancies (V_{Al}) were assumed to be decoupled in the present work and therefore were treated independently rather than as a cluster [$V_{Al}3O_{Cl}$]. In the expression for the segregation energy also, the bulk energies of the substitutional Cl and Al vacancies are subtracted separately (Eq. (1)). The depth of the scanning region to calculate the highest probability sites was between 2–4 Å for surfaces and 4–8 Å for GBs depending on the number of sites available in this region. The interfaces were divided into slabs of (0.5–1 Å) to reduce the number of possible Al vacancies for every triplet of Cl ions and hence, the number of possible permutations. For a certain triplet of Cl ions in a slab, an Al vacancy was created only in the same slab. Thereafter, the probabilities for Cl sites as well as Al vacancy sites were calculated as follows: $[\exp(\Delta E_i)/\Sigma\exp(\Delta E_i)]$. Where, ΔE_i is the energy of the site i (E_i) minus the energy of the farthest site from the interface. The probability of a specific multiple anion configuration was then estimated as the product of the probabilities of each occupied site as well as the vacancy. The lowest energy Cl sites and Al vacancy sites were permutated in order to get the lowest energy configurations of multiple Cl occupied alumina interfaces. In total 3 surfaces and 5 GBs were calculated, which are listed in Table 2. 150 configurations were calculated for each anion concentration.

Table 2
Sigma values of the twin grain boundaries, surface area (A) of the cells used for the calculations and interfacial energies of grain boundaries (γ_{GB}) and surfaces (γ_{surf}) calculated in the present work.

Miller index	Sigma (Σ)	A (nm^2)	γ_{surf} (J/m^2)	γ_{GB} (J/m^2)
(00.1)	3	0.77	2.99	2.66
(01.2)	7	0.70	2.62	0.27
(10.0)	3	0.59	2.80	0.50
(10.1)	11	0.62	3.67	1.88
(11.1)	93	1.03	3.48	2.87

The segregation energy of a configuration was calculated using the expression:

$$\Delta H_{seg}(N_{Cl}) = \frac{1}{N_{Cl}}\left(H(N_{Cl}) - H(0) - N_{Cl}\Delta H_{Cl,bulk} - \frac{N_{Cl}}{3}\Delta H_{V_{Al},bulk}\right) \quad (1)$$

where, $\Delta H_{seg}(N)$ is the segregation energy in the structure containing N Cl atoms. $H(N)$ is the potential energy of the structure containing N Cl atoms. $\Delta H_{i,bulk}$ is the change in enthalpy when inserting ion i or V_{Al} in the bulk, which was calculated by the Mott Littleton method with 4 Å and 10 Å as the radius of region 1 and 2 respectively.

Cl–Al coordination numbers and the nearest neighbor distances in the segregated interfaces were calculated to characterize the change in the atomic arrangement due to the presence of Cl impurities. The average distance of first nearest neighbor and second nearest neighbor was used as the cut off (4.25 Å) for these calculations.

3. Results and discussion

3.1. STEM-EDX analysis

Fig. 1a shows a high magnification bright field image of the transparent alumina sample. An equiaxed but non uniform grain growth was observed in the microstructure. Relatively straight GBs were identified and then tilted edge on to the electron beam for the EDX analysis of a single GB at a time (Fig. 1c). High magnification EDX analysis of the individual GBs showed the presence of Cl at the GBs and especially, high concentration of Cl ions was observed at the triple points (Fig. 1b). Bright contrast corresponding to the presence of Cl can be observed at the triple points as well as the GB in Fig. 1b. Because of the lower number of pixels and higher acquisition time in these maps a higher number of counts are collected, which makes it possible to see the Chlorine composition contrast.

Fig. 2 shows the results of EDX line scan analysis performed at three different locations of a single GB; two across the triple

Please cite this article in press as: Tewari A, et al. Segregation of anion (Cl^-) impurities at transparent polycrystalline α-alumina interfaces. *J Eur Ceram Soc* (2014), http://dx.doi.org/10.1016/j.jeurceramsoc.2014.04.018

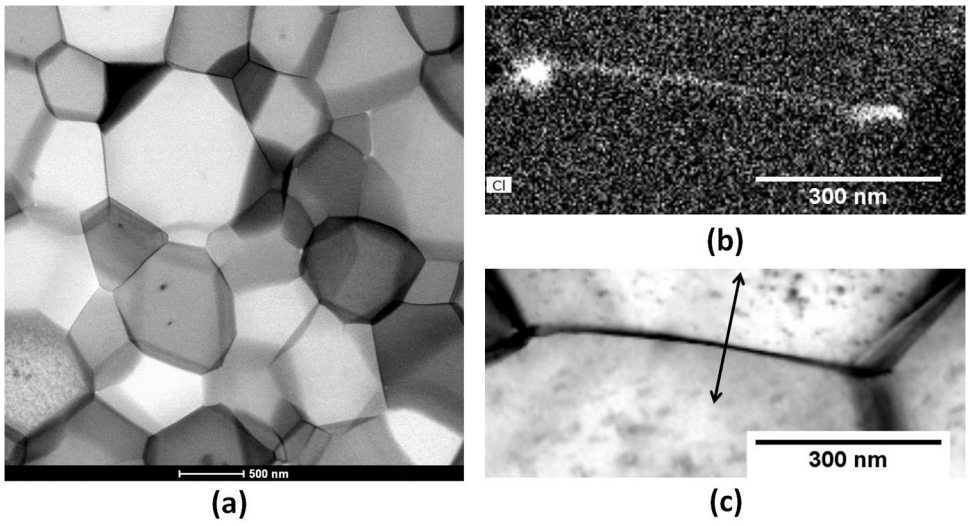

Fig. 1. (a) High magnification bright field image of alumina microstructure, (b) EDX analysis map showing the presence of Cl ion at the grain boundary and the triple points, (c) bright field image of a single edge-on grain boundary.

points and one across the GB (inset of Fig. 2). The significantly higher counts corresponding to the triple points in Fig. 2 show the preferable segregation of the Cl impurities to the triple points. The Cl peaks are observed in a narrow region centered on the GB plane (Fig. 2). Therefore, the Cl impurities are mostly concentrated only in the vicinity of the GBs and at the triple points as is also evident in the EDX maps shown in Fig. 1b. The EDX line scan analysis to determine the amount of anion impurities was done perpendicular to the GBs which were first tilted edge on to the electron beam. The line scan analysis showed large variation in the amount of Cl anions present at the GBs across the 7 analyzed GBs, ranging from 0.2 to 7.7 at./nm^2.

3.2. *Segregation energies* (ΔH_{seg})

Figs. 3 and 4 show the representative ΔH_{seg} versus anion concentration plots for the Cl segregated surfaces and GBs respectively. ΔH_{seg} for all the surfaces and GBs was found to be negative at all the calculated concentrations in the present work, which indicates that the Cl anion segregation is energetically favorable. ΔH_{seg} is slightly more negative for surfaces than GBs, which shows the higher tendency of segregation of anions to the surfaces. It might be attributed to the fact that it is easier to accommodate oversized anions on the surfaces than at GBs due to partially coordinated atoms at the interface.

ΔH_{seg} for Cl anions is 4–6 times more negative than the cation ΔH_{seg}, which is understandable given the much larger ionic size of Cl anions (3.62 Å) in comparison to La (1.17 Å) or Y (1.04 Å). Due to such a large size mismatch, the bulk solubility of Cl is expected to be very low in alumina and Cl is expected to strongly segregate to the interfaces. Such a strong segregation may result into a 'swamp out' effect, which is sometimes used to explain the reduced segregation of Mg in presence of Y.[19] It is essentially the inhibition of segregation of one cation dopant

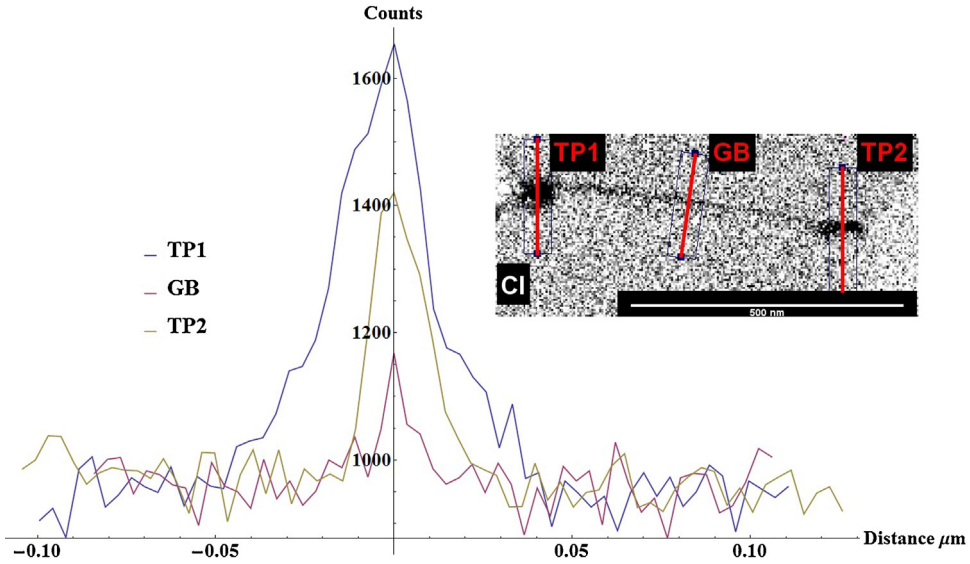

Fig. 2. Energy dispersive X-ray line scan analysis at three locations of a single grain boundary showing the peaks corresponding to the presence of Cl centered on the grain boundary plane. Zero value at the X-axis represents the grain boundary plane. The trajectories of the three line scans are shown in the inset.

Please cite this article in press as: Tewari A, et al. Segregation of anion (Cl^-) impurities at transparent polycrystalline α-alumina interfaces. *J Eur Ceram Soc* (2014), http://dx.doi.org/10.1016/j.jeurceramsoc.2014.04.018

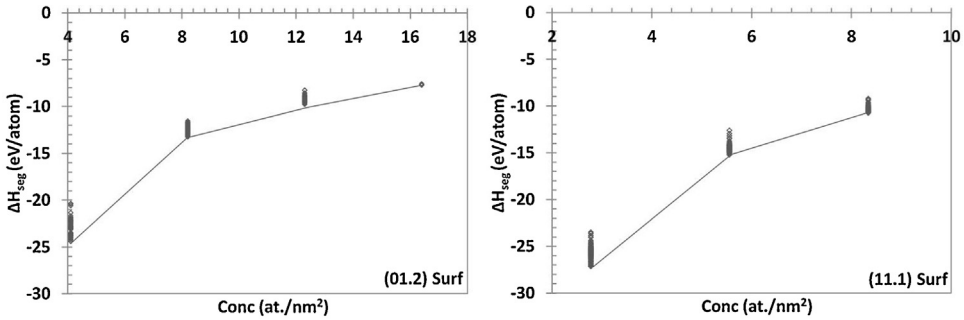

Fig. 3. Representative segregation energy (ΔH_{seg}) vs. surface impurity concentration plots for Cl segregation at (a) (01.2) and (b) (11.1) surfaces. Lines are just visual guides.

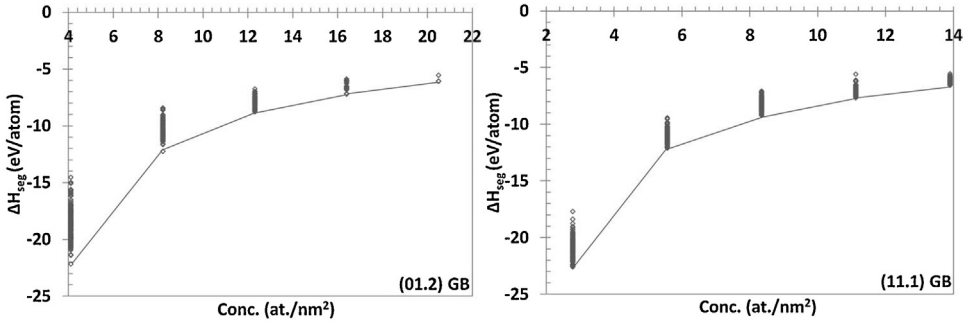

Fig. 4. Representative segregation energy (ΔH_{seg}) vs. grain boundary impurity concentration plots for Cl segregation at (a) (01.2) and (b) (11.1) grain boundaries. Lines are just visual guides.

due to the preferential segregation of other dopant. In this case very strong segregation of Cl anions may inhibit the segregation of other cation dopants at the GBs.

ΔH_{seg} continuously becomes more positive with the increasing anion concentration, which is similar to the majority of the cation doped interfaces However, one of the characteristics observed in the ΔH_{seg} versus concentration plots for the Cl anions is the discontinuity in slope of the curve at a certain concentration. The slope of the curve changes from a higher value to a lower value after a certain point. The discontinuity in slope of the segregation energy plot is the characteristic of a first order GB complexion transition at this concentration.[20] Table 3 gives the value of the characteristic concentration for first order GB complexion transition and minimum segregation energy at this concentration. The characteristic concentration varies significantly across the different interfaces, but it remains constant for the same index surface and GB. It should be noted here that in order to maintain the charge balance in the simulation cell, 1 Al vacancy needs to be created for every 3 Cl substituted atoms. Therefore, Cl atoms can be substituted only in the multiples of 3, which limit the allowed number of concentration points on the X-axis in Figs. 3 and 4. Hence, the exact characteristic concentration might be missed sometimes between the two calculated concentrations due to the large interval between them, which is different for each interface because of their different surface area. Interfacial atomic structures corresponding to this complexion transition will be discussed in the next section.

Table 3
Chlorine segregation energies are listed for alumina surfaces and GBs at the concentration corresponding to the first order grain boundary complexion transition. Corresponding characteristic concentrations are also given for each interface.

Miller index	Sigma (Σ)	Conc. (at./nm^2)	$\Delta H_{seg,surf}$ (eV)	$\Delta H_{seg,gb}$ (eV)
(00.1)	3	7.5	–	−12.3
(01.2)	7	8.2	−13.2	−12.2
(10.0)	3	9.8	−13.3	−10.9
(10.1)	11	9.3	–	−11.6
(11.1)	93	5.6	−15.2	−12.1

3.3. Interface atomistic structures

Fig. 5 shows the atomistic structure of the surfaces and the GBs at the characteristic concentrations as given in Table 3. It can be observed for all the interfaces that the formation of bilayer of the anions just begins at this concentration. Therefore, the characteristic concentration corresponds to the first order GB complexion transition of the interface from complexion I (single layer adsorption) to complexion III (bilayer adsorption) as described in Ref.21

Fig. 6 shows the evolution of the atomistic structure of a (11.1) GB with increasing dopant concentration. At the lowest dopant concentration (Fig. 6a), the Cl atoms are situated in a single layer at the GB. As the concentration increases the Cl atoms start occupying a bilayer at the GB. As the concentration increases further, multilayers and an intergranular film of anion impurity atoms are formed at the GB. According to the theory of complexion proposed by Harmer and coworkers,[21] the higher order GB complexions are observed as the concentration of Cl anions increases at the GBs.

Please cite this article in press as: Tewari A, et al. Segregation of anion (Cl^-) impurities at transparent polycrystalline α-alumina interfaces. *J Eur Ceram Soc* (2014), http://dx.doi.org/10.1016/j.jeurceramsoc.2014.04.018

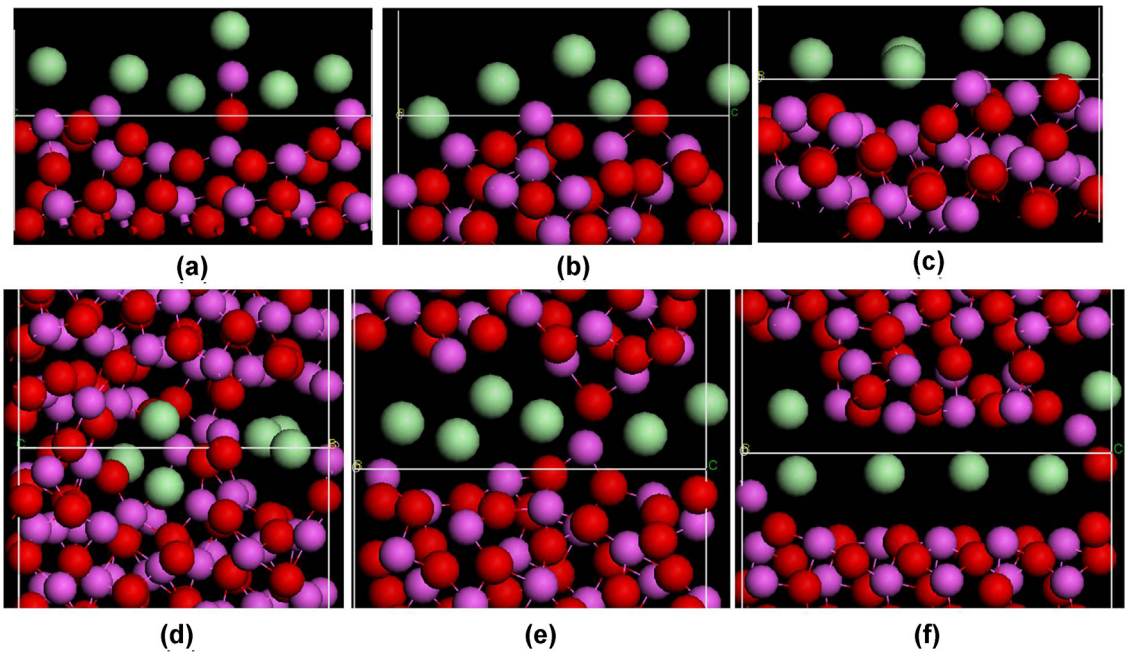

Fig. 5. Atomistic structures of the interface at their respective characteristic concentrations as mentioned in Table 2, (a) (01.2), (b) (10.0), (c) (11.1) surfaces, and (d) (11.1), (e) (10.1), (f) (01.2) grain boundaries. All the structures are seen parallel to the interface plane. Al atoms are in pink, Oxygen in red and Cl atoms are in green. (For interpretation of the references to color in this figure legend, the reader is referred to the web version of the article.)

Higher order complexions increase the GB mobility and mass transport.[21] Possibly anion impurities can cause the higher order complexions at lower concentrations than cation dopants due to their larger size. Combining this factor with the earlier discussed significantly higher segregation energies for anion segregation than cation dopants, may lead to the inference that anion segregation can increase the GB mobility and transport and hence, cause the enhanced grain growth at high temperatures nullifying the effect of cation dopants, as was observed by Dittmann et al.[13] during the sintering of Cl containing TiO_2 nano powders. Segregated oversized Cl anions at the GBs may also block the critical diffusive pathways (known as site blocking effect[22]), which will slow down the diffusion of the point defects (Al or O vacancies) across the GBs. Since the densification of alumina is controlled by the GB diffusion of point defects,[23] it will consequently slow down the densification of alumina. However, Roussel et al.[10] reported slightly higher densification of alumina with Chloride salts of dopants in comparison to nitrate salts. Therefore, further work needs to done to ascertain the comparative effect of the anion impurities on the GB diffusion of point defects in alumina.

3.4. Coordination numbers

The average Cl–Al coordination numbers (CN's) were calculated for different surfaces and GBs taking all the configurations at different concentrations into account, which are listed in Table 4. CN's for surfaces vary in the range of 4.3–4.9 (±2), while for the GBs the CN's vary from 6.4 to 8.6 (±4). The Cl–Al CN's for GBs are also very high in comparison to earlier observed CN 3 for GB O–Al atoms by Milas et al.[8] However, it should be noted that the variance in the calculated coordinate numbers are relatively large. α-Alumina has a hexagonal packed sub-lattice of oxygen with 2/3rd octahedral voids being occupied by Al atoms. In this arrangement of atoms CN of any O atom is less than or equal to 4 in the bulk alumina, while on a surface it should be 3 or less.[24] Higher coordination number of Cl than oxygen at the surface is an indication of stronger adhesion of Cl on the surface. In a recent study[13] on Cl segregation in TiO_2 also, it was suggested that chlorine is strongly bonded at the TiO_2 surface, which makes it difficult to release it at lower temperatures and therefore it may get entrapped into closed porosity during the densification process. Therefore higher concentrations of anion impurities should be expected at triple points. Comprehensive pore characterization study done by Stuer et al.[14] showed the existence of pores of approximately 50 nm in diameter at the triple points in the transparent polycrystalline alumina samples. However, the presence of these pores was attributed to the rapid spark plasma sintering, cationic dopants, and dislocations at high temperatures. The results from the microstructural study also support this observation, where STEM-EDX analysis confirmed the enhanced presence of Cl impurities at the triple

Table 4
Cl–Al coordination numbers of different interfaces are given with corresponding nearest neighbor distances.

Miller index	Surfaces		Grain boundaries	
	NN (Å)	CN	NN (Å)	CN
(00.1)	–	–	3.45	8.4
(01.2)	3.36	4.3	3.38	8.3
(10.0)	3.36	4.9	3.34	8.0
(10.1)	–	–	3.38	6.4
(11.1)	3.39	4.6	3.45	8.6

Please cite this article in press as: Tewari A, et al. Segregation of anion (Cl^-) impurities at transparent polycrystalline α-alumina interfaces. *J Eur Ceram Soc* (2014), http://dx.doi.org/10.1016/j.jeurceramsoc.2014.04.018

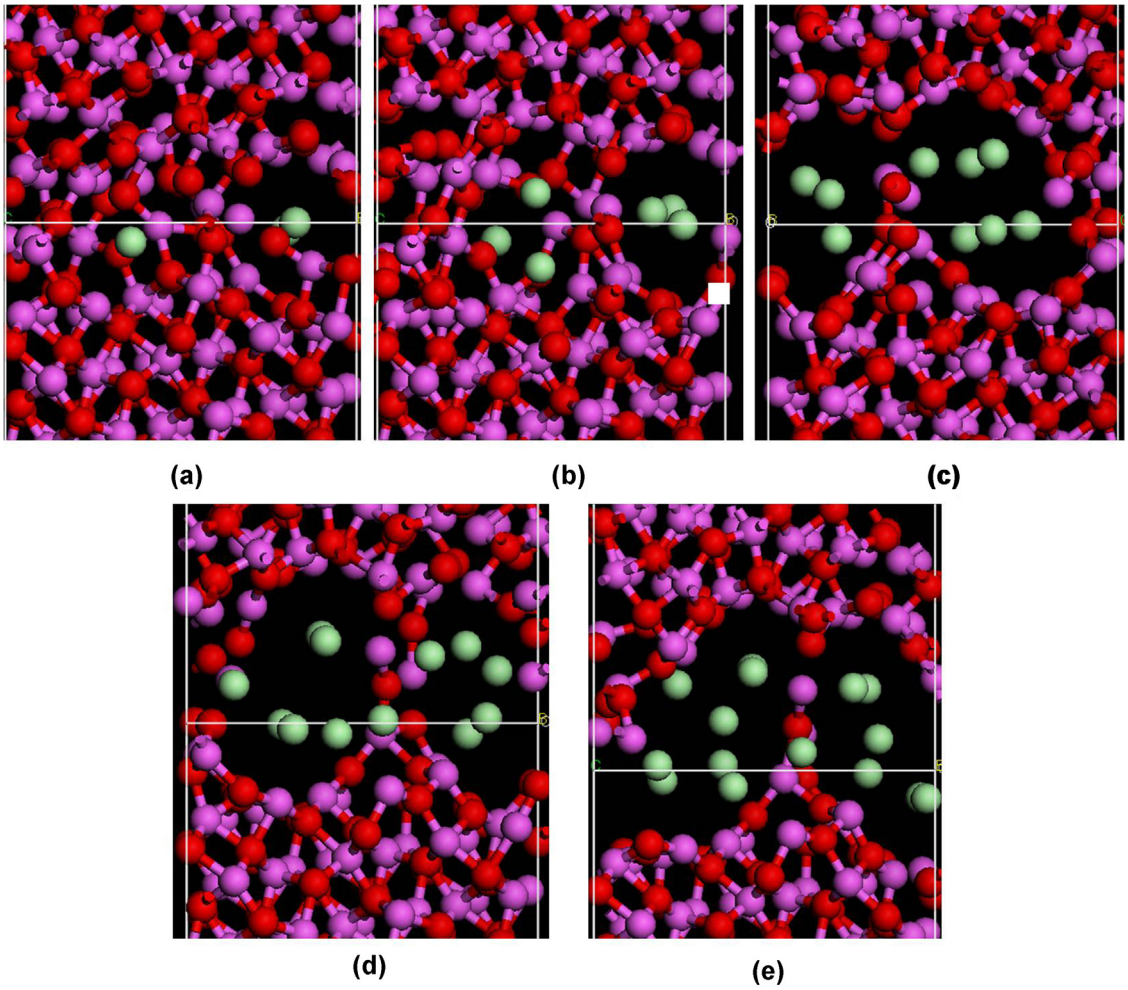

Fig. 6. Evolution of the atomistic structure of a (11.1) grain boundary with the increasing concentration of Cl ions, (a) 2.8 at./nm^2, (b) 5.6 at./nm^2, (c) 8.3 at./nm^2, (d) 11.11 at./nm^2, and (e) 13.90 at./nm^2. All the structures are seen parallel to the grain boundary plane. Al atoms are in pink, Oxygen in red and Cl atoms are in green. (For interpretation of the references to color in this figure legend, the reader is referred to the web version of the article.)

points (Section 3.1). Since the STEM-EDX analysis suggests the amount of Cl impurities to be approximately 250 ppm, perhaps some of the stable pores could be linked with Cl impurities and number of defects might be reduced with lower chlorine content.

Submicron size grains (<500 nm) and extremely low porosity with pore size less than 50 nm are the essential requirement for highly transparent alumina. Exaggerated grain growth would be very detrimental to the optical properties as it has been shown that the scattering depends on the largest characteristic scattering source (close to the dn90 of the pore size distribution).[14] The scattering from pores also depends on the characteristic size of the pores. But because of the high difference in refractive index between the pore and the alumina, the detrimental sizes for pores is much smaller (~50 nm).[12] If entrapped Cl at a pore surface (e.g. at the triple points) stops the pore from closing, then improvements in the RIT cannot be made with impurity levels seen in the powder used in the current study. A strategy to reduce the Cl content has to be investigated, e.g. chemical washing, or a modified powder synthesis method. Therefore, anion impurities may have similar effects as the non-desirable cation impurities (e.g. Si, Ca, Ti etc.), and should be taken into account when discussing the purity of alumna powders for transparent ceramic applications.

H_2O_2 can be used to clean the Chlorine impurities from surfaces. Therefore, a comparative study on sintering and microstructural properties of as received and H_2O_2 treated alumina powder should be conducted to experimentally study the effect of Cl on alumina properties

4. Summary and conclusions

The topic of segregation of anion impurities in alumina has been investigated for the first time using a combination of electron microscopy and atomistic modeling. STEM-EDX analysis at high magnification showed an enhanced concentration of Cl anion impurities at the triple points and varying concentration of Cl impurities at different GBs.

Atomistc simulations using energy minimization was used to calculate the segregation energy of the Cl anions at 3 surfaces and 5 different GBs. Strong segregation of the anion impurities to the surfaces and the GBs was predicted due to 4–6 times

Please cite this article in press as: Tewari A, et al. Segregation of anion (Cl^-) impurities at transparent polycrystalline α-alumina interfaces. *J Eur Ceram Soc* (2014), http://dx.doi.org/10.1016/j.jeurceramsoc.2014.04.018

higher segregation energies for the Cl anion in comparison to cation dopants previously studied (Mg, La, Y).

Segregation energy plots show a first order GB complexion transition at a certain concentration (6–10 atoms/nm^2) for each interface. Higher order GB complexions were observed with increasing impurity concentration, which would enhance GB mobility and mass transport and hence can result in exaggerated grain growth at high temperatures. This is of particular importance for transparent polycrystalline alumina where fine grains (<500 nm) and narrow size distributions are needed for high transmittances.

The coordination numbers (CN) of Cl–Al at the surfaces and GBs are higher than the O–Al CN. Higher Cl–Al CN at the surface suggest stronger adhesion of Cl on the surface. It would make the release of anion impurities at lower temperatures more difficult and they may get entrapped into the closed porosities and triple points, as was confirmed by the presence of Cl peaks away from the GBs in EDX line scan analysis. This can stabilize pores at sizes greater than the critical size where light scattering becomes important and small pore fraction can seriously deteriorate the optical properties in particular transmittance of light.

The present study has been able to demonstrate the importance of anion impurities present in alumina, which have been neglected so far in the processing of high purity alumina powders. The current results show the potential influence of anion impurities could be significant and needs to be taken into account especially for the processing of advanced ceramics where the margin for error is very small. Some of the propositions made in the present work based on the previous observations on other systems need to be confirmed with the experimental work focused on studying the effect of anions. Such as the use of H_2O_2 to clean the Chlorine impurities from surfaces.

Acknowledgements

The authors would like to thank the Swiss National Science Foundation SNF project No. 200020_144499 for the financial support for the current work.

References

1. Maki H, Takeuchi Y. Method for producing alpha-alumina particle. US7,858,067 B2; 2010.
2. Mirjalili F, Abdullah LC, Mohamad H, Fakhru'l-Razi A, Dayang Radiah AB, Aghababazadeh R. Process for producing nano-alpha-alumina powder. *ISRN Nanotechnol* 2011;**2011**:1–5.
3. Apetz R, Bruggen MPB. Transparent alumina A light-scattering model. *J Am Ceram Soc* 2003;**86**:480–6.
4. Krell A, Blank P, Ma H, Hutzler T, Nebelung M. Processing of high-density submicrometer Al_2O_3 for new applications. *J Am Ceram Soc* 2003;**86**:546–53.
5. Cannon RM, Rhodes WH, Heuer AH. Plastic deformation of fine-grained alumina (Al_2O_3): I. Interface-controlled diffusional creep. *J Am Ceram Soc* 1980;**63**:46–53.
6. Stuer M, Zhao Z, Aschauer U, Bowen P. Transparent polycrystalline alumina using spark plasma sintering: effect of Mg, Y and La doping. *J Eur Ceram Soc* 2010;**30**:1335–43.
7. Roussel N, Lallemant L, Chane-Ching J-Y, Guillemet-Fristch S, Durand B, Garnier V, et al. Highly dense, transparent α-Al_2O_3 ceramics from ultrafine nanoparticles via a standard SPS sintering. *J Am Ceram Soc* 2013;**96**:1039–42.
8. Milas I, Hinnemann B, Carter EA. Structure of and ion segregation to an alumina grain boundary: implications for growth and creep. *J Mater Res* 2008;**23**:1494–508.
9. Fan DH, Ding GQ, Shen WZ, Zheng MJ. Anion impurities in porous alumina membranes: existence and functionality. *Microporous Mesoporous Mater* 2007;**100**:154–9.
10. Roussel N, Lallemant L, Durand B, Guillemet S, Ching J-YC, Fantozzi G, et al. Effects of the nature of the doping salt and of the thermal pre-treatment and sintering temperature on Spark Plasma Sintering of transparent alumina. *Ceram Int* 2011;**37**:3565–73.
11. Lallemant L, Roussel N, Fantozzi G, Garnier V, Bonnefont G, Douillard T, et al. Effect of amount of doping agent on sintering, microstructure and optical properties of Zr- and La-doped alumina sintered by SPS. *J Eur Ceram Soc* 2014;**34**:1279–88.
12. Leipold MH, Kapadia CM. Effect of anions on hot-pressing of MgO. *J Am Ceram Soc* 1973;**56**:200–3.
13. Dittmann R, Wintermantel E, Graule T. Sintering of nano-sized titania particles and the effect of chlorine impurities. *J Eur Ceram Soc* 2013;**33**:3257–64.
14. Stuer M, Bowen P, Cantoni M, Pecharroman C, Zhao Z. Nanopore characterization and optical modeling of transparent polycrystalline alumina. *Adv Funct Mater* 2012;**22**:2303–9.
15. Galmarini S, Aschauer U, Bowen P, Parker SC. Atomistic simulation of Y-doped α-alumina interfaces. *J Am Ceram Soc* 2008;**91**:3643–51.
16. Galmarini S, Aschauer U, Tewari A, Aman Y, Van Gestel C, Bowen P. Atomistic modeling of dopant segregation in α-alumina ceramics: coverage dependent energy of segregation and nominal dopant solubility. *J Eur Ceram Soc* 2011;**31**:2839–52.
17. Tewari A, Galmarini S, Stuer M, Bowen P. Atomistic modeling of the effect of codoping on the atomistic structure of interfaces in α-alumina. *J Eur Ceram Soc* 2012;**32**:2935–48.
18. Binks DJ. *Computational modelling of zinc oxide and related oxide ceramics*. University of Surrey; 1994.
19. Nakagawa T, Sakaguchi I, Shibata N, Matsunaga K, Mizoguchi T, Yamamoto T, et al. Yttrium doping effect on oxygen grain boundary diffusion in [alpha]-Al_2O_3. *Acta Mater* 2007;**55**:6627–33.
20. Cantwell PR, Tang M, Dillon SJ, Luo J, Rohrer GS, Harmer MP. Grain boundary complexions. *Acta Mater* 2014;**62**:1–48.
21. Dillon SJ, Harmer MP. Demystifying the role of sintering additives with complexion. *J Eur Ceram Soc* 2008;**28**:1485–93.
22. Cho J, Wang CM, Chan HM, Rickman JM, Harmer MP. Role of segregating dopants on the improved creep resistance of aluminum oxide. *Acta Mater* 1999;**47**:4197–207.
23. Heuer AH. Oxygen and aluminum diffusion in [alpha]-Al_2O_3: how much do we really understand? *J Eur Ceram Soc* 2008;**28**:1495–507.
24. Tsyganenko AA, Mardilovich PP. Structure of alumina surfaces. *J Chem Soc Faraday Trans* 1996;**92**:4843–52.

Please cite this article in press as: Tewari A, et al. Segregation of anion (Cl^-) impurities at transparent polycrystalline α-alumina interfaces. *J Eur Ceram Soc* (2014), http://dx.doi.org/10.1016/j.jeurceramsoc.2014.04.018

Abhishek Tewari obtained his PhD degree in Materials Science and Engineering from Ecole Polytechnique Fédérale de Lausanne EPFL, Switzerland in 2013 and is currently doing a Postdoc at EPFL. His field of interest include atomistic modeling and simulation, transparent ceramics and tribology of ceramics.

Farhang Nabiei is a graduate student in the institute of materials science at EPFL since 2013. He obtained his master degree in materials science from EPFL in 2013. Currently his graduate research focus is electron microscopy characterization.

Marco Cantoni is a research and teaching staff in the Interdisciplinary Center for Electron Microscopy (CIME) at EPFL. He obtained his PhD from ETH Zurich, Switzerland in 1993 in the field of experimental physics. His field of expertise include TEM, high resolution TEM, SEM, FIB, STEM and several other electron microscopy characterization techniques.

Paul Bowen is a senior scientist at the Powder Technology Laboratory, EPFL. He obtained his PhD from University of Cambridge in Physical Chemistry in the field of catalysis in 1982. His main research interests are powder synthesis, powder characterisation, colloidal processing, sintering of ceramics and atomistic modelling of surfaces and interfaces.

Cécile Hébert is the director of the Interdisciplinary Center for Electron Microscopy (CIME) and associate professor at EPFL. She obtained her PhD degree (design of a new energy filter for transmission electron microscopy, under the direction of Prof. B. Jouffrey) at the Ecole Centrale in Paris. Her main research interests are Computational Electron Microscopy, Angular resolved Electron Energy Loss Spectrometry, STEM-EELS and three dimensional imaging and Chemical Analysis.

Please cite this article in press as: Tewari A, et al. Segregation of anion (Cl^-) impurities at transparent polycrystalline α-alumina interfaces. *J Eur Ceram Soc* (2014), http://dx.doi.org/10.1016/j.jeurceramsoc.2014.04.018